



## Determination of the potential byproduct in the toluene oxidation process by $\text{CuMnO}_x$ catalyst on cordierite substrate

Tran Thị Thu Hien<sup>2,3</sup>, Vu Duc Hiep<sup>1</sup>, Nguyen Van Chuc<sup>1</sup>, Khong Manh Hung<sup>1</sup>, Ly Bích Thuy<sup>2</sup>, Le Minh Thang<sup>1\*</sup>

<sup>1</sup>School of Chemical Engineering, Ha Noi University of Science and Technology, 01 Dai Co Viet, Ha Noi, Viet Nam

<sup>2</sup>School of Environmental Science and Technology, Ha Noi University of Science and Technology, 01 Dai Co Viet, Ha Noi, Viet Nam

<sup>3</sup>Faculty of Natural Sciences, Quy Nhon University, 170 An Duong Vuong, Quy Nhon City, Binh Dinh, Viet Nam

\*Email: [thang.leminh@hust.edu.vn](mailto:thang.leminh@hust.edu.vn)

### ARTICLE INFO

Received: 17/9/2021

Accepted: 21/10/2021

Published: 22/10/2021

#### Keywords:

$\text{CuMnO}_x$ , toluene, impregnation method, by-products

### ABSTRACT

Cordierite is the substrate that possesses a low thermal expansion coefficient, good thermal shock resistance, excellent mechanical properties, and chemical resistance. Thus, cordierite is widely used as substrate for catalysts in high-temperature applications like gaseous treatment.  $\text{CuMnO}_x$ /cordierite catalyst for the complete oxidation of toluene was prepared by the impregnation method and characterized by XRD, BET, IR techniques. This work evaluated the catalytic activity of the prepared catalyst at the temperature range from 150°C to 350°C. It was found that  $\text{CuMnO}_x$ /cordierite catalyst completely converted toluene to  $\text{CO}_2$  at 350°C. In addition, the mechanism of the toluene oxidation process using  $\text{CuMnO}_x$ /cordierite catalyst was also determined via the identification of the presentation of the by-products by GC/MS technique at various reaction temperature of 200°C, 250°C, and 350°C. The results showed that the reaction over the  $\text{CuMnO}_x$ /cordierite catalyst followed the same mechanism as proposed by Lars and Andersson. The intermediate products of the oxidation process at 200°C, 250°C, and 350°C were benzyl alcohol, benzaldehyde, benzoic acid, benzene, phenol, 1,4-hydroquinone, 1,4-benzoquinone, and maleic anhydride.

### Introduction

Manganese oxide is one of the active catalysts for oxidation of CO and VOCs, e.g. toluene, at a relatively low cost. Therefore, it has recently attracted considerable scientific research and application in the industry. It is also a component of the Hopcalite catalyst system that continues to be investigated until today. Mn-based oxides can be classified into some

oxide forms depending on the preparation conditions:  $\text{MnO}$ ,  $\text{MnO}_2$ ,  $\text{Mn}_2\text{O}_3$ ,  $\text{Mn}_3\text{O}_4$ . Their properties and application of manganese oxide catalysts are influenced by the crystal structure, morphology, surface area, and grain size [1].

The structure of manganese based oxide contains many lattice oxygens instability. Therefore, it is possible to store oxygen in the crystal lattice and improve CO

and VOC oxidation process. The catalytic activity of manganese base catalysts depends on the oxidation states of manganese.

In recent years, several studies have been conducted to estimate the ability to remove VOCs such as n-hexane [2], benzene [3], toluene [4], and so on. The efficiency of the oxidation process using manganese oxide-based catalyst depends on the catalyst synthesis method, experimental conditions, and oxidation states of manganese [5]. The catalyst has high-efficiency oxidation due to the presence of  $Mn^{2+}/Mn^{3+}$ ,  $Mn^{3+}/Mn^{4+}$ . Moreover, the activity of the Mn-based catalyst for the oxidation of ethyl acetate and n-hexane were even higher than that of the Pt/TiO<sub>2</sub> catalyst [6]. Besides, the combination of manganese oxide and transition metal oxide has been studied to enhance the catalytic activity for gaseous pollutant treatment.

Copper – Manganese oxide catalysts were one of the mixed transition metal oxide catalysts that were widely used in CO and VOCs oxidation at room temperature [7,8,9,10].

Morales and coworkers investigated the role of Cu-Mn mixed oxides catalyst in the propane oxidation process [11]. They showed that this catalyst had higher conversion propane to CO<sub>2</sub> at lower temperatures than pure manganese or copper oxide. Besides, Ntainjua and Taylor demonstrated that the oxidation activity catalyst was involved reducibility and surface area [12]. Geunino et al. investigated aromatic VOCs oxidation performance of copper manganese oxide catalyst. In this study, the catalysts exhibited the highest catalytic activity for the oxidation of toluene compared to benzene, ethylbenzene, and xylene [13].

Supported catalysts are also investigated in many studies and applied in the industry [14,15]. An example is the study of Einaga et al. about CuMnO<sub>x</sub> supported on SiO<sub>2</sub>. In this investigation, the catalyst exhibited the most significant activity in benzene oxidation related to the CuMn<sub>2</sub>O<sub>4</sub> and Cu<sub>2</sub>Mn<sub>3</sub>O<sub>8</sub> phases [5]. In the study of Tsoncheva et al., the activity catalyst was improved due to dispersing Cu and Mn particles into the porous structure of SBA-15 support [16]. According to Feng et al., the interaction between manganese and copper in the CuMn mixed oxides catalysts on TiO<sub>2</sub> was the main factor that created the high activity of the catalyst [17]. However, these powder supports are not suitable for industrial application.

Cordierite (2MgO–2Al<sub>2</sub>O<sub>3</sub>–5SiO<sub>2</sub>) is the material that consists of magnesium aluminosilicate with a hexagonal framework. Cordierite is often applies for high-

temperature processes due to its low thermal expansion coefficient, good thermal shock resistance, excellent mechanical properties, and chemical resistance [18,19].

These properties were the main factors determining the role of cordierite as the substrate in the pollutant gas treatment system [20].

Our previous research showed that CuMnO<sub>x</sub> powder has a high activity for toluene oxidation at 250°C [21]. However, the powder catalysts could cause clogged pipe entirely, so there was much difficult to apply the kind of catalyst in reality. Thus, the CuMnO<sub>x</sub>/cordierite catalyst was studied for application in gaseous treatment systems. The present work focused on investigating the ability of CuMnO<sub>x</sub>/cordierite system for the complete oxidation of toluene, which can apply for industrial gas treatment. The catalytic activity of the catalyst was evaluated, and the byproducts of the reaction were identified by GC-MS technique to understand the oxidation mechanism.

## Experiment

### *Preparation of the catalysts*

Copper manganese mixed oxide catalyst on cordierite was synthesized by the impregnation method. Mn(NO<sub>3</sub>)<sub>2</sub> 50% solution was added to a Cu(NO<sub>3</sub>)<sub>2</sub> solution with a molar ratio of 1/2 ( $Mn^{2+}/Cu^{2+}$ ) under stirring and heating to 50°C for 2hrs. Cordierite was also added into the solution and impregnated for 1h. The impregnated cordierite was dried at 110°C for 1h then calcinated at 300°C for 3hrs at the rate of 3°C/min.

The impregnation process was repeated five times to get more CuMnO<sub>x</sub> on the cordierite surface. Finally, the solid was calcined at the rate of 2°C/min to 500°C and remained for 3hrs. The obtained catalyst consisted of 37 percent of the activated phase.

The remaining solution after the impregnation process was dried at 120°C for 1h and calcined at 500°C for 3hrs at a heating rate of 2 min/°C. The catalyst was assigned as CuMnO<sub>x</sub> powder.

### *Catalyst characterization*

The BET surface area was determined by N<sub>2</sub> adsorption-desorption isotherms by a Micromeritics Gemini VII 2390 device. X-ray diffraction (XRD) pattern was measured by the D8 Advance Bruker instrument.

Infrared spectra (IR) were characterized by the Nicolet IS50 FT – IR spectrometer.

### Catalytic oxidation experiment

The catalysts were evaluated for the oxidation reaction of toluene using a fixed bed reactor system. The sample (0,1 g) was loaded in a micro stainless steel reactor that was 60 cm in length. An N<sub>2</sub> flow went through a toluene bubbler before going to the reactor. When the inlet toluene flow reached a steady state at 5000 ppm, the reaction was started. The reaction temperature was increased from 150°C to 350°C. The amount of toluene in reactant flow was analyzed by an online gas chromatography (GC) using a Thermal Conductivity Detector (TCD). Toluene and the products of the reaction (CO<sub>2</sub>, H<sub>2</sub>O, by-product) at 200°C were analyzed by GC Trace 1310 equipped with MS ISQ700 system, using the CP-SilicaPLOT column 30 m x 0.32 mm with the temperature program: remain at 35°C for 4 minutes, increase with a rate of 10°C /min to 190°C, and remain for 5 minutes.

### Analysis and calculation of the result

Toluene conversion was evaluated by the equation 1:

$$\eta_T (\%) = \frac{C_T^1 - C_T^2}{C_T^1} \times 100 \quad (1)$$

Where,  $\eta_T$ : toluene conversion (%);

$C_T^1$ : toluene concentration of inlet flow at a temperature T (ppm);

$C_T^2$ : toluene concentration of outlet flow at a temperature T (ppm).

The conversion of toluene to CO<sub>2</sub> was determined as equation 2:

$$\gamma_{CO_2} (\%) = \frac{C_{CO_2, T}^2}{7(C_T^1 - C_T^2)} \times 100 \quad (2)$$

Where,  $\lambda_{CO_2}$ : the conversion of toluene to CO<sub>2</sub> (%);

$C_{CO_2, T}^2$ : CO<sub>2</sub> concentration of outlet flow at a temperature T (ppm);

## Results and discussion

### Characterization of the catalyst

The surface of cordierite with and without impregnation of CuMnO<sub>x</sub> active phase was observed by using a optical microscope with 4x magnification (Fig 1). The surface of fresh cordierite consists of large particles. After impregnation, it was covered by the

catalyst phase CuMnO<sub>x</sub> with a small particle size that changed the surface to dark color. The images of the catalyst showed that the CuMnO<sub>x</sub> catalyst was successfully impregnated on cordierite.



Figure 1: The magnification image of the CuMnO<sub>x</sub> supported on cordierite

The CuMnO<sub>x</sub> powder possesses BET surface of 10.72 m<sup>2</sup>/g. Besides, the BET surface of cordierite was minimal [21], and the BET surface of CuMnO<sub>x</sub>/cordierite catalyst was 1.92 m<sup>2</sup>/g. Thus, cordierite was excellent substrate due to the thermal resistance, but its BET surface was small, therefore, it doesn't play the role to distribute active sites so the content of the active site on cordierite substrate should be as much as possible since a decrease in the desorption of the activated phase on the cordierite substrate has been observed [20]. Therefore, in this study, the impregnation process was repeated many times to get more CuMnO<sub>x</sub> on the cordierite surface.

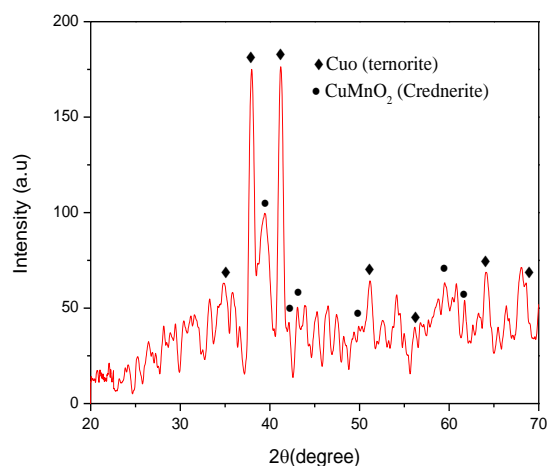


Figure 2: XRD pattern of CuMnO<sub>x</sub> powder

In order to determine phase composition of CuMnO<sub>x</sub> catalyst, the CuMnO<sub>x</sub> powder was characterized by the XRD technique. The XRD pattern of the catalyst was featured by the diffraction peaks at 2θ: 32.34°; 35.6°; 38.8°; 48.86°; 53.82°; 61.62°; 66.12° corresponding to the lattice (110), (002), (111), (202), (020), (113), (311) [17]

of crystal structure tenorite CuO respectively [22]. The XRD also illustrated the structure of crednerite CuMnO<sub>2</sub> at 2 $\theta$  values of 36.94°; 39.68°; 40.64°; 59.38°; 53.3°; 61.7°; 66.2° corresponding to the (110), (20-2), (111), (31-1) [23-25]. Therefore, the main phases of catalyst were the tenorite CuO and the crednerite CuMnO<sub>2</sub>

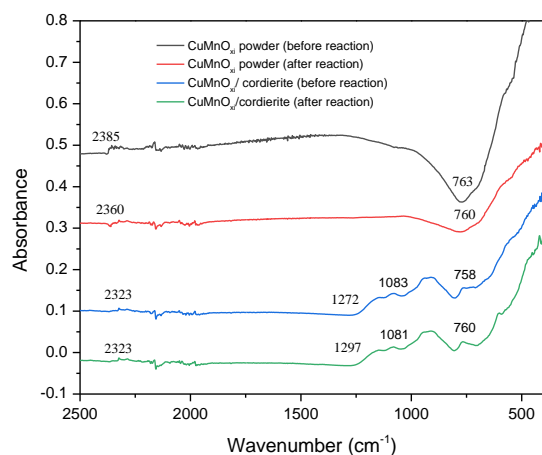


Figure 3 : IR profile of catalysts.

Figure 3 illustrated IR spectra of CuMnO<sub>x</sub> powder and CuMnO<sub>x</sub>/cordierite catalysts. In the spectra of CuMnO<sub>x</sub> powder and CuMnO<sub>x</sub>/cordierite before and after the reaction, the vibration at the wavenumber between 400 to 800 cm<sup>-1</sup> belong to manganese oxides [25]. For the CuMnO<sub>x</sub>/cordierite catalysts, the vibrations appearing at 736 and 759 cm<sup>-1</sup> indicated the tunnel structure's Mn–O bond and the bands at 1081 and 1083 cm<sup>-1</sup> for the Mn<sup>3+</sup> - O bond [26].

The CuMnO<sub>x</sub>/cordierite catalysts presented an evidence of a CO<sub>3</sub><sup>2-</sup> group at 1237 and 1297 cm<sup>-1</sup>, and wave number at 2323 cm<sup>-1</sup> in the CuMnO<sub>x</sub>/cordierite and CuMnO<sub>x</sub> powder catalysts indicated the presence of the C=O group due to the absorbed CO<sub>2</sub> on their surface [27]. IR spectra showed no difference between catalysts before and after the toluene oxidation reaction.

### Catalytic activity

The experiment results of the toluene oxidation process on the prepared catalysts are described in Fig. 4 and Figure 5

The results showed that when the temperature of the oxidation process increased from 150°C to 350°C, the toluene conversion and the CO<sub>2</sub> yield increased. In Fig 4, the CuMnO<sub>x</sub> powder catalyst indicated the highest toluene conversion at 300°C, while the CuMnO<sub>x</sub>/cordierite catalyst showed a complete toluene conversion at 350°C.

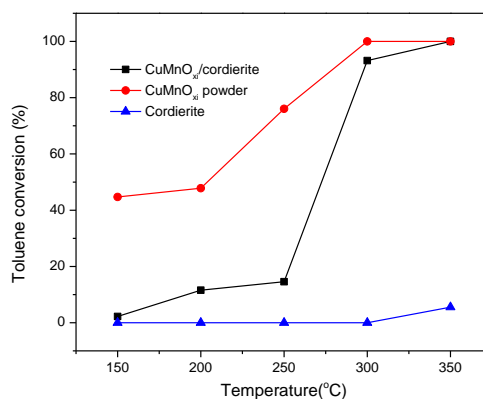


Figure 4: Toluene conversion

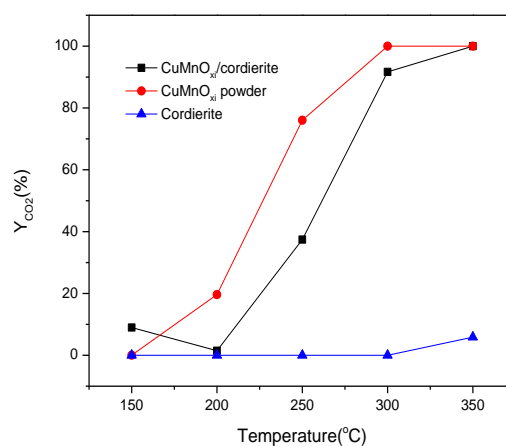


Figure 5: CO<sub>2</sub> yield

At almost reaction temperature, the conversion of toluene and CO<sub>2</sub> yield of CuMnO<sub>x</sub> powder were higher than that of CuMnO<sub>x</sub>/cordierite catalyst. Moreover, bare cordierite showed zero conversion of toluene and CO<sub>2</sub> yield at low temperature and very low activity at 350°C. It means that the activity of CuMnO<sub>x</sub> powder and CuMnO<sub>x</sub>/cordierite come from CuMnO<sub>x</sub> phase. Besides, CuMnO<sub>x</sub>/cordierite catalyst had only 37 percent of the active phase. Therefore, it is observed that toluene conversion and yield of CO<sub>2</sub> are rated to the catalyst's active phase concentration.

### Determination of the products by GC/MS technique

According to the literature [28-34], the intermediate products of toluene oxidation are benzyl alcohol, benzaldehyde, benzoic acid, benzene, phenol, 1,4-Hydroquinone, 1,4-Benzoquinone, and Maleic anhydride. The reaction scheme was proposed by Lars and Andersson (Fig 6). Therefore, we try to define the products during the oxidation reaction by GC-MS to

insight into the oxidation reaction mechanism with the CuMnO<sub>x</sub>/cordierite catalyst

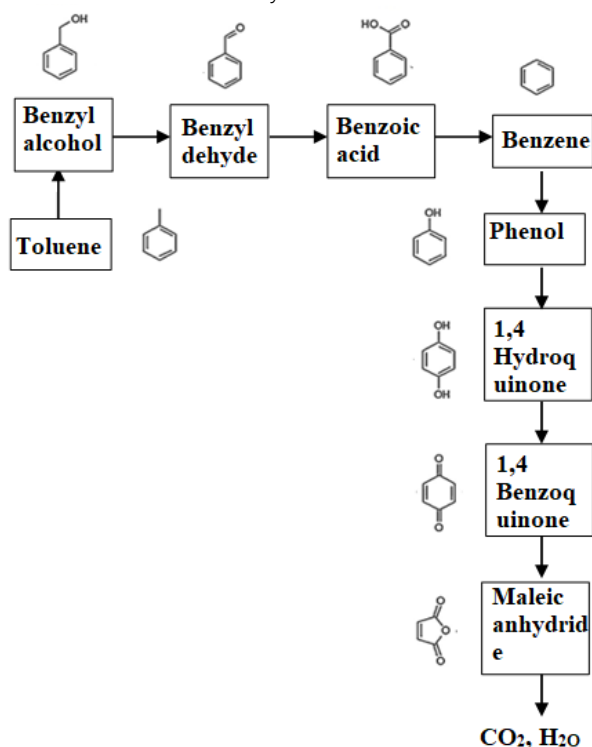


Figure 6: The byproducts were proposed by Lars and Andersson [32]

Table 2 listed the mass spectrometry of possible intermediate products in the proposed mechanism according to the literature. Main and unique mass fragments (marked in bold in Table 2) are followed by the GC-MS analysis program.

Table 2: The by-products were observed by mass spectrometry

No	Substance	RT	The mass fragments in relative intensity order
1	Benzyl alcohol	1.11 – 1.95	108> <b>107</b> >79>77>91>90>51>50
2	Benzaldehyde	1.11 – 1.95	<b>106</b> >105>77>51>50>52>78
3	Benzoic acid	1.11 – 1.95	105> <b>122</b> >77>51>50>52
4	Benzene	1.11 – 1.95	<b>78</b> >>77>51>50>52
5	Phenol	1.11 – 1.95	<b>94</b> >>66>65>39
6	1,4-Hydroquinone	1.11 – 1.95	<b>110</b> >>81>82>55>53
7	1,4-Benzoquinone	1.11 – 1.95	108>54>26>82> <b>80</b>
8	Maleic alhydride	1.11 – 1.95	54>26>> <b>98</b> >53>25

The analysis was performed for the toluene oxidation process on the CuMnO<sub>x</sub>/cordierite catalysts at 200°C, 250°C and 350°C. The trends of formed products are presented in Fig 7. It is shown that all of the products

suggested in the reaction scheme proposed by Lars and Andersson was found in the outlet gas flow.

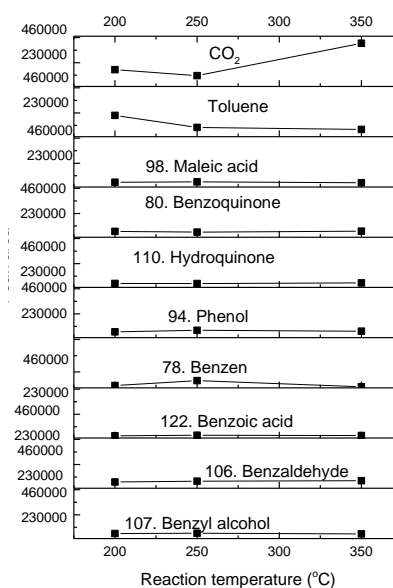


Figure 7: Trend of the products in the toluene oxidation process between 200°C and 350°C

In Fig 7, we could observe the product trend in the toluene oxidation process from 200°C and 350°C. The products: benzyl alcohol, benzene, benzoic acid, phenol, maleic acid, 1,4 hydroquinone, 1,4 benzoquinone presented in small quantities and seems not change when the temperature increase from 200 to 350°C. Moreover, Fig.7 showed a general profile of a significant amount of produced carbon dioxide- as a function of temperature. CO<sub>2</sub> increase significantly from 200°C to 350°C. While there was a sharp drop in toluene concentration from 200°C to 350°C. However, the concentration of unconverted toluene is still higher than the concentration of above mentioned byproducts. Since the sensitivity of the GC-MS is much higher than for the GC with TCD detector, it was found that a small amount of toluene was still detected in the outlet gas flow even it was found 100% converted as seen from the GC-TCD.

## Conclusion

This study showed that although possessing lower active phase than the powder catalyst, CuMnO<sub>x</sub>/cordierite catalyst can completely oxidate converter toluene to CO<sub>2</sub> at 350°C, which is suitable to apply in industry. The catalyst is also thermal and mechanical stable at high temperatures. The GC/MS technique was used to determine toluene, CO<sub>2</sub>, H<sub>2</sub>O, and intermediate products such as benzyl alcohol,

benzaldehyde, benzoic acid, benzene, phenol, 1,4-hydroquinone, 1,4- benzoquinone, and maleic anhydride of the toluene oxidation process. The results demonstrated that the toluene oxidation process followed well the mechanism proposed by Lars and Andersson. The intermediate products are still present in the outlet gas after the reaction at high temperature but with low concentration. The reaction will be investigated in more detail in the following study to improve the catalyst's performance.

## Acknowledgments

Tran Thi Thu Hien was funded by Vingroup Joint Stock Company and supported by the Domestic Master/ PhD Scholarship Programme of Vingroup Innovation Foundation (VINIF), Vingroup Big Data Institute (VINBIGDATA), VINIF.2020.TS.80.

The authors thank the supports of VJC, VINIF, VINBIGDATA.

Moreover, this work has been supported by the RoHan Project funded by the German Academic Exchange Service (DAAD, No. 57315854) and the Federal Ministry for Economic Cooperation and Development (BMZ) inside the framework "SDG Bilateral Graduate school programme"

The authors thank the supports of Rohan project, DAAD, BMZ, Laboratory of Petrochemical Refining and Catalytic materials, Laboratory of Environmental Friendly Material and Technologies, HUST.

## References

1. M. S. Kamal, S. A. Razzak, M. M. Hossain, *Atmospheric Environment* 140 (2016) 117-134. <https://doi.org/10.1016/j.atmosenv.2016.05.031>
2. C. Lahousse, A. Bernier, E. Gaigneaux, P. Ruiz P, P. Grange, B. Delmon, *Proceedings of the 3rd World Congress on Oxidation Catalysis 1997* 777-785. [http://doi.org/10.1016/s0167-2991\(97\)81040-3](http://doi.org/10.1016/s0167-2991(97)81040-3)
3. J. Luo., Q. Zhang, A. Huang, S. L. Suib, *Microporous and Mesoporous Materials*, 35 (2000), 209-217. [http://doi.org/10.1016/s1387-1811\(99\)00221-8](http://doi.org/10.1016/s1387-1811(99)00221-8).
4. F. N. Aguero, A. Scian, B. P. Barbero, L. E. Cadús., *Catalysis Today* 133 (2008) 493-501. <http://doi.org/10.1016/j.cattod.2007.11.044>
5. H. Einaga, S. Yamamoto, N. Maeda, Y. Teraoka, *Catalysis Today*, 242 (2015) 287-293. <http://doi.org/10.1016/j.cattod.2014.05.018>
6. Q. Sun, L. Li, H. Yan, X. Hong, K.S. Hui, Z. Pan, *Chemical Engineering Journal* 242 (2014) 348-356. <http://doi.org/10.1016/j.cej.2013.12.097>
7. L.Naleki, M. Haghshenas Frad, M. Khoshnoodi, A. A. Mirzaei, G. J. Hutching, S. H. Taylor, *Iranian Journal of Chemical Engineering* 1 (2004) 11 -18.
8. S. Behar, P. Gonzalez, P. Aguilhon, F. Quignard, D. Swierczyński, *Catalysis Today* 189 (2012) 35-41. <https://doi.org/10.1016/j.cattod.2012.04.004>
9. B. D. Napruszewska, A. Michalik, A. Walczyk, D. Duraczyńska, R. Dula, W. Rojek, L. Lityńska-Dobrzyńska, K. Bahrnowski, E. M. Serwicka, *Materials* 11 (2018). <https://doi.org/10.3390/ma11081365>
10. T. J. Clarke, S. A. Kondrat, S. H. Taylor, *Catalysis Today* 258 (2015) 610-615.
11. M. R. Morales, B. P. Barbero, L. E. Cadús, *Applied Catalysis B: Environmental* 67 (2006) 229-236. <http://doi.org/10.1016/j.apcatb.2006.05.006>.
12. N. E. Ntainjua, S. H. Taylor, *Topics in Catalysis*, 52 (2009) 528-541. <https://doi.org/10.1007/s11244-009-9180-x>.
13. H.C. Genuino, S. Dharmarathna, E.C. Njagi, M.C. Mei, S.L. Suib, *The Journal of Physical Chemistry C* 116 (2012) 12066-12078. <https://doi.org/10.1021/jp301342f>
14. R. G. Akay, A. B. Yurtcan, *Direct Liquid Fuel Cells: Fundamentals, Advances and Future*, Elsevier 2020 <https://doi.org/10.1016/C2018-0-04168-7>.
15. G. Allen, J.C. Bevington, *Comprehensive polymer science and supplements*, Elsevier, 1996, <https://doi.org/10.1016/B978-0-08-096701-1.00181-6>.
16. T. Tsoncheva, G. Issa, I. Genova, M. Dimitrov, *Journal of Porous Materials* 20 (2013) 1361-1369. <https://doi.org/10.1007/s10934-013-9722-2>.
17. D. Fang, J. Xie, D. Mei, Y. Zhang, F. He, X. Liu, Y. Li, *RSC Advances* 4 (2014). <https://doi.org/10.1039/c4ra02824d>
18. N. R. E. Radwan, G. A. El-Shobaky, Y. M. Fahmy, *Applied Catalysis A: General* 274 (2004) 87-99. <https://doi.org/10.1016/j.apcata.2004.05.032>.
19. M. Rundans, G. Sedmale, I. Sperberga, I. Pundiene, *Advances in Science and Technology* 89 (2014) 94-99. <http://doi.org/10.4028/www.scientific.net/as>
20. T. M. P. Phạm, Q. M. Nguyễn, T.T. Nguyễn, I. Van Driessche, M.T. Lê, *Investigating the different*

- methods of cordierite's preparation to apply in three-way catalysts manufacture, *Materials* 50(2012), 135 – 138.  
<https://doi.org/10.3390/ma7096237>
21. T. T. H. Tran, B. T. Ly, T. M. P. Pham, M. T. Le, *Vietnam Journal of Catalysis and Adsorption*, 10 (2021).  
<https://doi.org/10.51316/jca.2021.068>
  22. D. MubarakAli, J. Arunkumar, P.Pooja, G. Subramanian, N. Thajuddin, N. S. Alharbi, *Saudi Pharmaceutical Journal* 23 (2015) 421–428.  
<http://doi.org/10.1016/j.jsps.2014.11.007>.
  23. D. Zhu, L. Wang, W.Yu, H.Xie, *Scientific reporters* 8(2018).  
<https://doi.org/10.1038/s41598-018-23174-z>
  24. N. Benreguia., A. Barnabé, M. Trari, *Materials Science in Semiconductor Processing* 56 (2016) 14 – 19.  
<http://doi.org/10.1016/j.mssp.2016.07.012>.
  25. L. Wang, M. Arif, G. Duan, S. Chen, X. Liu, *Journal of Power Sources* 355 (2017) 53–61.  
<http://doi.org/10.1016/j.jpowsour.2017.04.05>.
  26. L. Cai, Z. Hu, P. Branton, W. Li W, *Chinese Journal of Catalysis* 32 (2014) 159–167.  
[http://doi.org/10.1016/s1872-2067\(12\)60699-8](http://doi.org/10.1016/s1872-2067(12)60699-8).
  27. L. Kang, M. Zhang, Z. H. Liu, K. Ooi, *Spectrochimica Acta Part A: Molecular and Biomolecular Spectroscopy*, 67 (2007) 864–869.  
<http://doi.org/10.1016/j.saa.2006.09.001>.
  28. S. Dey, G. C. Dhal, D. Mohan, R. Prasad, *Bulletin of Chemical Reaction Engineering & Catalysis*, 12 (2017) 393–40.  
<http://doi.org/10.9767/bcrec.12.3.882.393-407>.
  29. Z. Tian., W. J. Pitz, R. Fournet, P. A. Glaud, F. Battin - Leclerc, *Proceedings of the Combustion Institute* 33 (2011) 233–241.  
<http://doi.org/10.1016/j.proci.2010.06.063>
  30. Y. Ji, J. Zhao, H. Terazono, K. Misawa, N. P. Levitt, Y. Li, ... R. Zhang, *Proceedings of the National Academy of Sciences* 114 (2017), 8169–8174.  
<http://doi.org/10.1073/pnas.1705463114>
  31. J. A. A. Hoorn, P. L. Alsters, G. F. Versteeg, *International Journal of Chemical Reactor Engineering* 3 (2005).  
<http://doi.org/10.2202/1542-6580.1196>
  32. R. Wu, S. Pan, Y. Li, L. Wang (2014), *The Journal of Physical Chemistry A* 118 (2014) 4533–4547.  
<http://doi.org/10.1021/jp500077f>
  33. S. L. T. Andersson, *Journal of Chromatographic Science* 23 (1985) 17–21.  
<http://doi.org/10.1093/chromsci/23.1.17>
  34. G. Xiao, W. Xu, R. Wu, M. Ni, C. Du, X. Gao, Z. Y. Luo, K. Cen, *Plasma Chemistry and Plasma Processing* 34 (2014) 1033–1065.  
<http://doi.org/10.1007/s11090-014-9562-0>
  35. X. Li, J. Xu, F. Wang, J. Gao, L. Zhou., G. Yang, *Catalysis Letters* 108 (2006) 137–140.  
<https://doi.org/10.1007/s10562-006-0034-x>